Synthesis of Cobalt Ferrite Nanocomposite Coated with Aluminum Oxide and Application in Protein Removal Process in Natural Rubber

Vu Thi Thuy[1,2], Le Thi Thu Trang[2], Dao Ngoc Thi[1], Nguyen Nhat Trang[1],
Le Thi Hong Nhung[1], Nguyen Thai Huy[1], Phan Trung Nghia[1]*

[1]*School of Chemistry and Life Sciences, Hanoi University of Science and Technology, Ha Noi, Vietnam*
[2]*Rubber Science and Technology Center, Hanoi University of Science and Technology, Ha Noi, Vietnam*

Abstract

Proteins in latex are the main cause of unwanted effects for users, such as skin allergies and unpleasant odors. Therefore, it is necessary to remove protein from rubber latex before putting it into production. The study presents a method and process for synthesizing $CoFe_2O_4$ (CFO) magnetic nanoparticles coated on the surface with an Al_2O_3 coating. Then, based on the surface adsorption mechanism of the Al_2O_3 coating, the protein in the latex is adsorbed and recovered from the solution by the magnetism of the CFO magnetic core. The CFO material synthesized by the co-precipitation method has an evenly distributed spherical shape, size 27.3 nm, from a saturation of 53.9 emu/g. The synthesized $CFO@Al_2O_3$ has an evenly distributed spherical shape, size 56.2 nm, from a saturation of 39.07 emu/g, and a surface area of 216.75 m^2/g. The $CFO@Al_2O_3$ nanoparticles have the ability to separate proteins up to 96.71% and have been researched and proven by the Kjeldahl method.

Keywords: Aluminum oxide, cobalt ferrite, nanocomposite, natural rubber, protein.

1. Introduction

Natural rubber (NR) is a polymer material with outstanding properties such as water resistance, excellent electrical insulation, significant elongation, high elasticity, green tensile strength and environmental friendliness, used to produce medical products, household appliances and industrial equipment. However, surgical gloves and medical devices made from NR can cause immediate allergic reactions such as respiratory failure and anaphylaxis (e.g., angioedema, urticaria, and cyanosis). That allergy is caused by proteins - a specific type of Ig E antigen found in NR [1]. The structure of NR and the protein separation process in NR are shown in Fig. 1.

The protein removal process is mainly carried out by two methods, namely using urea together with surfactant (U-DPNR de-protein natural rubber by urea) or using enzyme (E-DPNR de-protein natural rubber by enzyme) [2]. The proteins not only exist in the aqueous phase but also bind to the surface of rubber particles. Rubber particles with a diameter of 0.5-3µm are surrounded by a layer of negatively charged phospholipid protein. This layer is about 20nm thick and has a complex structure. Some studies show that the layer surrounding rubber particles also reduces the reactivity of rubber molecules when performing denaturation reactions. Reactive agents (radicals, anions, cations) are inhibited in the presence of a protein layer [3]. Therefore, the removal of proteins is

necessary to expand the application of this material. The protein removal process from high ammonia natural rubber (HANR) is shown in Fig. 2.
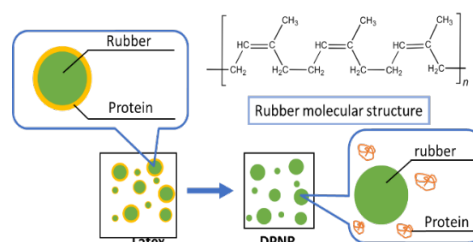
Fig. 1. NR separates proteins
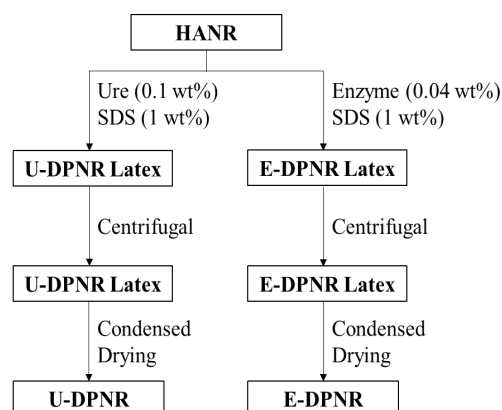
Fig. 2. Protein removal process in NR latex

Currently, the method of protein separation in NR is widely used, which is urea annealing method combined with sodium dodecyl sulfate (SDS) surfactant. This method removes protein to 92.89% (the nitrogen content in natural latex is 0.38% after protein separation by urea annealing method, the remaining nitrogen content in latex is about 0.027%) [4]. However, this method needs to be done in batches, which is time-consuming and energy-intensive during centrifugation. Therefore, it is necessary to find new methods to shorten the time and consume less energy. Currently, there has been research on the method of removing proteins in natural rubber latex by the adsorption mechanism of hollow nanocomposite materials.

On the other hand, CFO nanomaterials with special properties such as superparamagnetism, low toxicity, good dispersion in synthetic dispersions easily have potential applications in many biomedical fields such as cell extraction, immunoassay, drug conduction, local hyperthermia. With external magnetic field control, CFO nanoparticles are currently being investigated to separate proteins in natural latex by functionalizing their core-shell surface with a coating of Al_2O_3 porous material.

In the classification of magnetic materials, CFO is classified as ferrite materials as a group of magnetic materials with the general formula $MO.Fe_2O_3$ and has a spinel structure, where M is a 2-valent metal such as Fe, Ni, Co, Mn, Zn, Mg or Cu. In this material, oxygen ions have a radius of about 1.32Å which is much larger than the radius of metal ions (0.6-0.8 Å) so they are located very close to each other and arranged into a lattice with a tightly arranged face-centered cubic structure. The $MO.Fe_2O_3$ molecular structure is shown in Fig. 3.

In this network, there are vulnerabilities of two types: the first is the tetrahedral hole (group A) limited by 4 oxygen ions, and the second is the octahedral hole (group B) limited by 6 oxygen ions. M^{2+} and Fe^{3+} metal ions will be located in these holes and form two types of spinel structures of the ferrite material group. In the spinel structure, half of the Fe^{3+} ions and all M^{2+} ions are at position B, and the remaining half of the Fe^{3+} ions are at position A. Ferromagnetic material $CFO = CoO$. Fe_2O_3 is a ferrite with a typical converse spinel structure [5].

Aluminum oxide is the chemical compound of aluminum and oxygen with the chemical formula Al_2O_3. It is also known as alumina in the mining, ceramics and materials scientific community. Aluminum oxide is a white, insoluble solid that does not react with water. Melting at very high temperatures (above 2000 °C), has a coefficient of thermal expansion of $0.063K^{-1}$ [6]. The Al_2O_3 molecular structure is shown in Fig. 4.

Fig. 3. $MO.Fe_2O_3$ molecular structure (https://next-gen.materialsproject.org/materials/mp-765860/)

Fig. 4. Al_2O_3 molecular structure (https://next-gen.materialsproject.org/materials/mp-1938/)
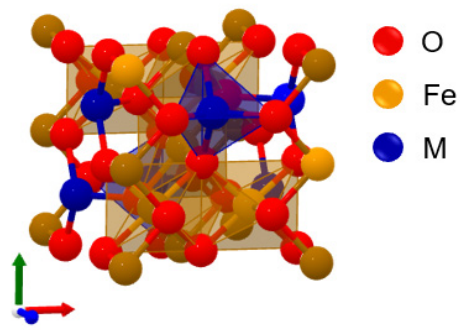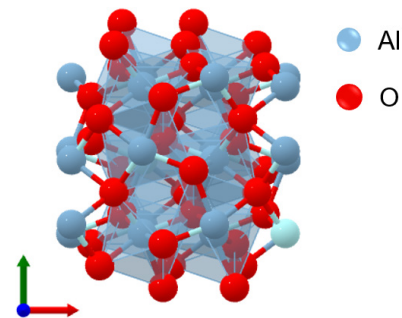
It has been proven that the formation of passivating coatings of inert materials such as organic polymers or inorganic materials on the surface of CFO nanoparticles can help prevent their agglomeration during dispersion, and improve their chemical stability. To overcome the limitations, magnetic core-shell nanoparticles with CFO as core and shell as metal oxide or metals such as gold, silica, titania and alumina are widely proposed. Among them, aluminum-coated CFO nanoparticles are of interest due to their low cost, high biocompatibility, chemical stability, high surface area, good electrical conductivity, and ease of synthesis. Due to the above properties of the aluminum oxide shell and the unique magnetic properties of the CFO core, $CFO@Al_2O_3$ nanoparticles have proven to be simple, inexpensive and effective materials for protein immobilization.

In this study, results were achieved when removing proteins from natural rubber using magnetic nano $CFO@Al_2O_3$ in the presence of a surfactant. Natural latex combined with SDS surfactant causes the protein chains to separate from the rubber molecule and break dispersed in latex, based on the surface adsorption mechanism of the material $CFO@Al_2O_3$ the broken protein chains will enter the capillary pores on the surface of the material and be recovered by the magnetism of the CFO magnetic core by the external magnetic field.

2. Experiment

2.1. Chemicals

Natural rubber latex used in this work is high ammonia natural rubber provided from Dau Tieng Rubber latex Co, Ltd. Sodium dodecyl sulfate (SDS, 99 %), Selen (Se, 99%), Potassium sulfate (K_2SO_4, 98%) and Copper sulfate (Cu_2SO_4, 98%) were purchased from Chameleon Reagent (Japan). Urea (99.5 %) and Boric acid (H_3BO_3, 99%) were obtained from Nacalai-Tesque (Japan). Sodium hydroxide (NaOH, 97%) was purchased from Fisher (England). Aluminium nitrate nonahydrate ($Al(NO_3)_3$, 98.5%), Iron(III) chloride nonahydrate ($FeCl_3.9H_2O$) and Cobalt(II) chloride hexahydrate ($CoCl_2.6H_2O$, 98%) were purchased from Sigma-Aldrich.

2.2. Synthesis of CFO@Al₂O₃

2.2.1. Synthesis of cobalt ferrite nanoparticles by the co-precipitation method

To synthesize magnetic nanoparticles with high dispersibility in water, we first slowly pour the mixture containing $FeCl_3$ and $CoCl_2$ into NaOH solution under continuous magnetic stirring conditions for 60 minutes. The return of the salt mixture to a highly concentrated alkaline solution allows the creation of a batch of crystalline particles, while limiting the rate of seed growth, helping to form precipitated precursor particles with very high efficiency small size. During agitation, the pH solution is kept stable about 11-13 for 2 hours. After the synthesis, the seeds are washed several times with distilled water until the pH value of 7 is reached.

2.2.2. Synthesis of nanocomposite cobalt ferrite coated with aluminum oxide

The CFO nanoparticles are coated with aluminum hydroxide by surface precipitation reaction. A solution of $Al(NO_3)_3.9H_2O$ 1M is slowly added to the CFO particle reactor system at a drip rate of about 5ml/min. The pH value of the solution is adjusted to 8.0 by adding a 2M NaOH solution. The mixture is stirred within 2 hours after adding the solution (without using magnetic stirring), the stirring rate is adjusted to 500 rpm. During the reaction, the temperature is maintained at 80°C.

After harvesting, the seeds will be washed several times with distilled water until the pH reaches a value of 8.0. Next, the resulting grain is calcined at 450 °C, 500 °C, 550 °C, 600 °C, 650 °C for 2 hours. The material obtained after firing for 2 hours will be transformed into CFO@Al₂O₃.

2.3. Protein Removal in Natural Rubber

High-ammonium natural rubber (HANR) contained approximately 60% dry rubber content (DRC) and a fine mesh filter to eliminate all impurities in latex. It is then converted into natural rubber with DRC x% (x=10, 15, 20, 25, 30) by mixing with distilled water and adding 0.1 wt.% SDS. Stirred the solution well for 15 minutes to obtain latex 1. The pH of latex 1 was then adjusted to 11 using NH₄OH 5%. Next, an amount of CFO@Al₂O₃ equal to 1wt.% was added to the latex solution (latex 2). This mixture was stirred with a mechanical stirrer for 30 minutes. Protein type separation process using CFO@Al₂O₃ is shown in Fig. 5.
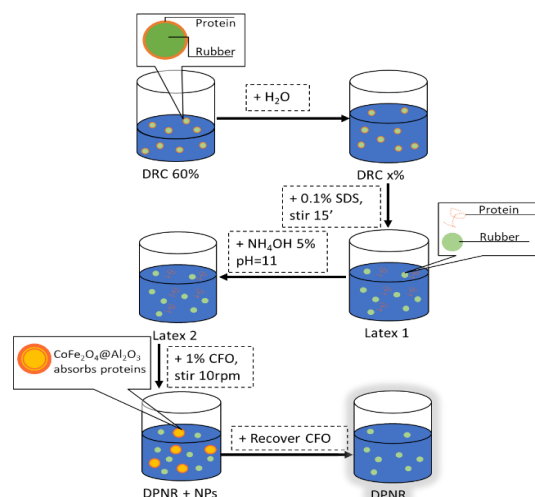
Fig. 5. Protein type separation process using CFO@Al₂O₃

To recover CFO@Al₂O₃ nanoparticles in DPNR, use rare earth magnets for separation and recovery. Finally, use the resulting latex solution to form a film and dry it at 50 °C.

2.4. Characterization Methods

The characterization of the prepared cobalt ferrite nanoparticles was conducted by using various techniques to verify the particle size and distribution and to explore other parameters of interest. The structure of the $CoFe_2O_4@Al_2O_3$ nanoparticles was characterized by the XRD technique using a Shimadzu diffractometer (model XRD 6000) with Cu Kα (0.154nm) radiation to generate diffraction patterns from the crystalline powder samples at ambient temperature over the 2θ range from 20° to 80°. The average sizes of CFO and CFO@Al₂O₃ crystals are calculated using the Scherrer formula [7]:

$$D = \frac{0.94\lambda}{\beta_{hkl}\cos\theta} \quad (1)$$

D: is the crystal particle size at the angular position θ

λ: is the wavelength of X-rays (1.54178Å)

β_{hkl}: is the semi-width (FWHM) of pic featured on the XRD, radian, spectrum.

θ: is the angle of irradiation

The scanning electron microscope (SEM) images were used to determine the surface morphology of the synthesized CFO@Al$_2$O$_3$ (SEM, JEOL JSM-7600F). Magnetic characterization of the cobalt ferrite nanoparticles was performed by using a vibrating sample magnetometer (VSM) (Lake Shore 4700) at room temperature with a maximum magnetic field of 15 kOe [7]. The specific surface area was determined by BET (Brunauer–Emmett–Teller) method in Tristar 3000 (Micromeritics - USA).

Nitrogen content was determined by Kjeldahl method [8]. Exactly 0.1g dried rubber was mixed with 0.65 g catalyst consisting of Potassium Sulfate, Copper Sulfate and Selenium in the mass ratio 15:02:01 and 2.5 ml of concentrated sulfuric acid (H$_2$SO$_4$ 98%). Then this mixture was burned under the flame of an alcohol lamp for a period of 30-40 minutes until a homogeneous solution changed to a light green color. The decomposition product was alkalized with NaOH solution and distilled in excess of boric acid (H$_3$BO$_3$). Titration was done with 0.01N H$_2$SO$_4$ acid standard solution with the methyl red as indicator.

3. Results and Discussion

3.1. X-ray Diffraction Measurement (XRD) Results

The X-ray diffraction diagram of CFO, CFO@Al$_2$O$_3$ materials (600°C, 2h) is shown in Fig. 6. The results show that the diffraction diagram of CFO powder samples has peaks at $2\theta = 30.25°$, $35.71°$, $43.48°$, $54.21°$, $57.43°$, $63.10°$, $74.95°$ corresponding to the lattices (220), (311), (400), (422), (511), (440), (622) of CFO crystals with cubic structure.

The diffraction diagram of CFO@Al$_2$O$_3$ powder samples (600 °C, 2h) has diffraction peaks at 2θ corresponding to the characteristic peaks of CFO crystals, in addition to peaks at $2\theta = 39°$, $45.71°$, $66.6°$ corresponding to lattices (222), (311), (422) of Al$_2$O$_3$.

This demonstrates that the synthesis of CFO is completely successful and contains no impurities and the synthesis is CFO@Al$_2$O$_3$ successful because of the presence of the peak of Al$_2$O$_3$ in the X-ray diffraction scheme of CFO@Al$_2$O$_3$.

From the above results, we can calculate the average size of CFO and CFO@Al$_2$O$_3$ crystals at the diffraction peak (311), which are 27.3 nm, 56.2 nm, respectively. Thus, using the synthesis method in this paper, nano-sized materials have been synthesized.

3.2. SEM Imaging Results

The morphology of CFO and CFO@Al$_2$O$_3$ materials is presented in the Fig. 7, Fig. 8. The SEM image shows that nm-sized particles are fairly evenly distributed. The average particle sizes of CFO and CFO@Al$_2$O$_3$ materials are 27.82 nm and 58.3 nm respectively, which is in accordance with the crystal size results calculated from XRD measurement.
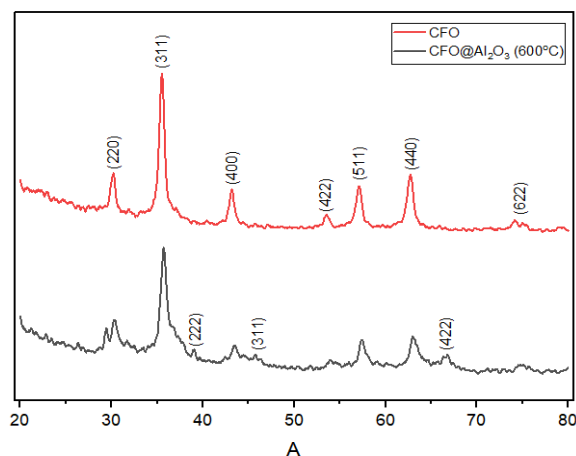
Fig. 6. XRD pattern of CFO and CFO@Al$_2$O$_3$
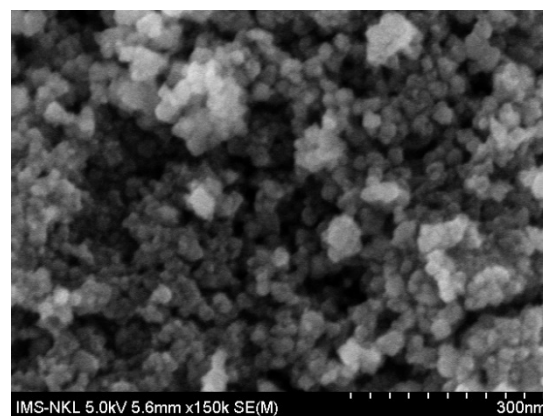
Fig. 7. CFO SEM image
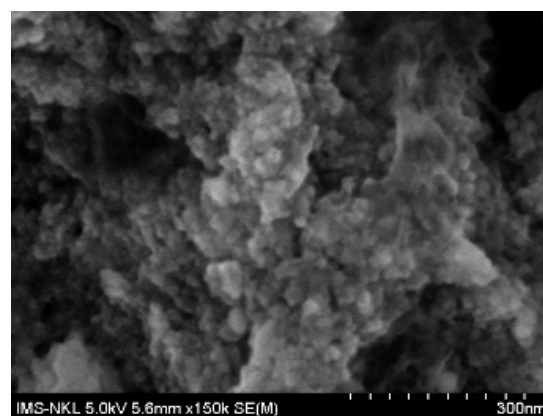
Fig. 8. SEM image of CFO@Al$_2$O$_3$

3.3. BET Surface Area Results

The specific surface area of the material is measured using the BET method. The specific surface areas of CFO@Al$_2$O$_3$ (500 °C, 2h) and CFO@Al$_2$O$_3$ (600 °C, 2h) materials at room temperature are shown in the Table 1.

From the results in Table 1, we see that the specific surface area of the CFO@Al$_2$O$_3$ increased from 83.55 m^2/g to 216.75 m^2/g when the firing temperature was increased from 500 °C to 600 °C.

This result shows that with a heating temperature of 500 °C in 2 hours, the CFO@Al(OH)$_3$ material has been formed and the material has not reached the desired CFO@Al$_2$O$_3$ material with absolute porous structure. With a firing temperature of 600 °C, the product has reached the porous state of the Al$_2$O$_3$ material, the pores have a diameter of about 30-120Å, and the pore volume is 0.5 - 1 cm^3/g. The surface area depends on both the firing temperature and firing time.

3.4 Magnetic Measurement Results (VRM)

The results of VSM magnetic measurement at room temperature of CFO (drying at 80 °C) and CFO@Al$_2$O$_3$ (heating at 600 °C for 2h) samples are shown in Fig. 9.

The results of the survey of magnetic properties such as: antimagnetic force, magnetic saturation, residual magnetism, square numerator are specifically presented in Table 2.

The results of the survey of the dependence of magnetism on the external magnetic field showed that the CFO material obtained by the co-precipitation method is a soft magnetic material. When enveloped with Al$_2$O$_3$, the resistance from H_c and saturate magnetization M_s decreases. Based on the results of the resistance from H_c and saturate magnetization M_s of the CFO sample and the granular CFO@Al$_2$O$_3$ sample, we see that the resistance from the obtained H_c decreased from 627 Oe for CFO to 207 Oe for CFO@Al$_2$O$_3$, saturate magnetization M_s decreased from 53.49 emu/g for CFO to 39.07 emu/g for CFO@Al$_2$O$_3$.

Using the co-precipitation method, CFO nanoparticles were synthesized. X-ray diffraction results indicate that the CFO particles produced are nano-sized, monophase, and fall under the ferrite materials category. VSM analysis results reveal that the saturation of the CFO@Al2O3 sample is notably lower than that of the uncoated CFO sample.

3.5. Effect of Reaction Time, Heating Temperature and %DRC on Nitrogen Content in NR

3.5.1. Effects of reaction time

We perform a protein separation reaction using CFO@Al$_2$O$_3$ material (calcined at 600°C for 2h) with the following reaction conditions: % dry rubber content (%DRC) = 30%, %SDS = 0.1wt.%, pH=11, % nanoparticles (%NPs) = 1wt.%, reaction time changes t = 15, 30, 45, 60, 75 minutes. The nitrogen content in rubber latex after separation was determined using the Kjeldahl method, as shown in Fig. 10.

Table 1. BET measurement results

No.	Sample	Specific surface area (m^2/g)
1	CFO@Al$_2$O$_3$ (500°C, 2h)	83.55
2	CFO@Al$_2$O$_3$ (600°C, 2h)	216.75

Table 2. Magnetic resistance and saturate magnetization of the material

No.	Sample	H_c(Oe)	M_s(emu/g)
1	CFO	627	53.49
2	CFO@Al$_2$O$_3$	207	39.07
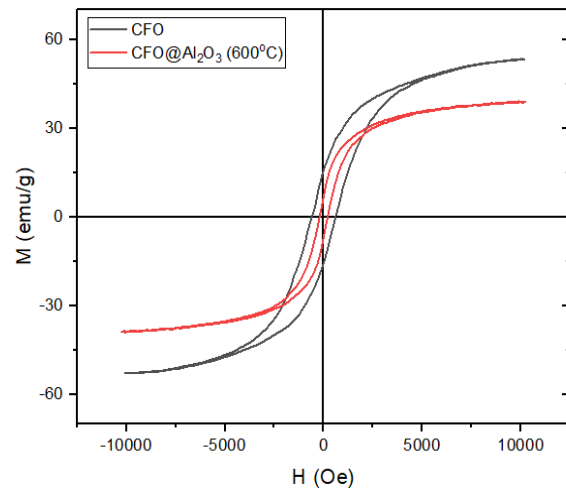
Fig. 9. Vibration sample magnetometer (VSM) measurement results
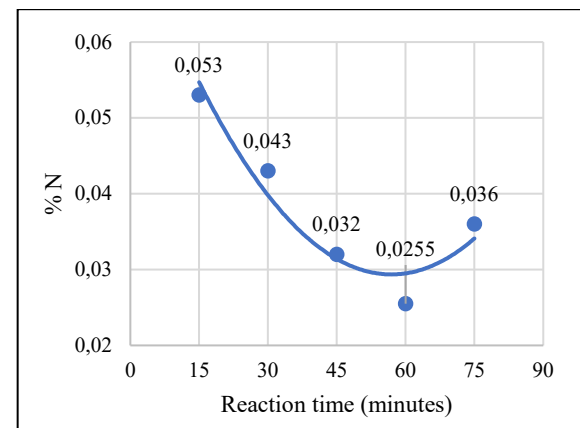
Fig. 10. Effect of reaction time

Based on the graph results, changing the reaction time will affect the total nitrogen content. The extreme point of the graph is at the reaction time of 60 minutes and the total nitrogen content of 0.0255%. It was shown that the best protein removal occurred with a reaction time of 60 min. Therefore, we will choose a reaction time of 60 minutes to further investigate the influencing factors.

3.5.2. Effect of CFO@Al₂O₃ calcination temperature

In the next survey, we perform the protein separation reaction using CFO@Al₂O₃ materials with different heating temperatures (calcined at 450 ºC, 500 ºC, 550 ºC, 600 ºC, 650 ºC for 2 hours) with reaction conditions following: %DRC = 30%, %SDS=0.1wt.%, pH = 11, %NPs = 1wt.%, reaction time t=60 minutes (optimal conditions drawn from the first survey). The nitrogen content in rubber latex after separation was determined using the Kjeldahl method, as shown in Fig. 11.

From the results on the diagram, we come to the observation that the heating temperature of the material CFO@Al(OH)₃ affects the properties of the material and the ability of the material to separate the protein type (total nitrogen content). The extreme point of the graph is where the CFO@Al(OH)₃ calcination temperature at 600ºC and the total nitrogen content is 0.025%. It was shown that with a firing temperature of 600 ºC for 2 hours, CFO@Al₂O₃ material has the ability to separate proteins in NR latex most optimally. Therefore, we will use CFO@Al₂O₃ material heated at 600ºC to conduct further influencing factor surveys.
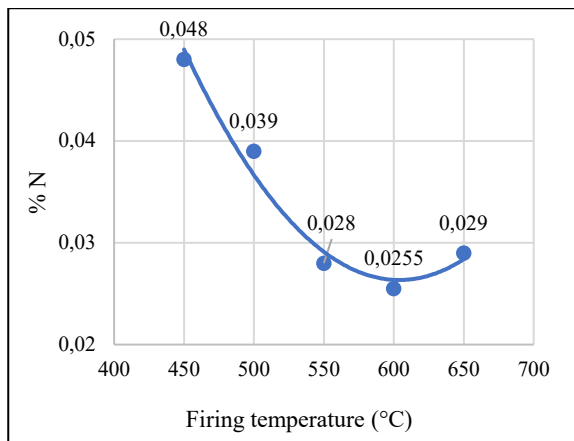
Fig.11. Effect of firing temperature

3.5.3. Effect of %DRC

In the next survey, we perform a protein separation reaction using CFO@Al₂O₃ materials (calcined at 600 ºC for 2 hours) with the following reaction conditions: %SDS = 0.1wt.%, pH = 11, %NPs=1wt.%, reaction time t= 60 minutes and will change the dry rubber content in the solution %DRC = 30%, 25%, 20%, 15%, 10%. The nitrogen content in rubber latex after separation was determined using the Kjeldahl method, as presented in Fig. 12.
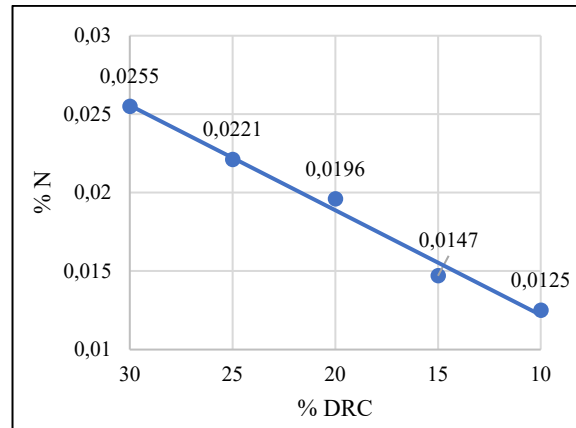
Fig. 12. Effect of %DRC

From the results, we can see that %N in rubber increases as the content of dry rubber (%DRC) increases. This suggests that the ability of NPs to split proteins decreases as the rubber concentration gets thicker. This relationship shows that there is a positive correlation between %DRC and %N in rubber. When the dry rubber content in rubber increases, the nitrogen content also tends to increase. This can be explained as follows: Based on the adsorption mechanism, we can also imagine that the higher density (concentration) of the adsorbed substance in the solution, the lower adsorption capacity, proportional to concentration.

3.5.4. Comparison with the protein separation method using urea

Rubber samples prepared for comparison include: NR that has not been deproteinized (HANR), NR that has been deproteinized by Urea incubation according to the procedure below (U-DPNR) and NR that has been deproteinized using CFO@Al₂O₃ material (600 ºC, 2h synthesized in the study under optimal separation conditions (DPNR by NPs).

From the results of Comparing the protein separation efficiency between urea annealing (U-DPNR) and separation method by CFO@Al₂O₃ nanomaterials (DPNR by NPs), we find that the protein separation process with urea results is quite good, reaching 92.89% of the total nitrogen content (nitrogen content decreased from 0.38% in unseparated NR latex to 0.027% in DPNR).

Table 3. Comparison with type separation method

No.	Sample	Nitrogen (%)
1	HANR	0.38
2	U-DPNR	0.027
3	DPNR by NPs	0.012

However, the method of protein separation by nanoparticles, CFO@Al$_2$O$_3$ gave a better effect, reaching 96.71%, the total nitrogen content (nitrogen content decreased from 0.38% in unseparated NR latex to 0.012% in DPNR by NPs). This proves that the removal of proteins in NR latex by nanoparticles CFO@Al$_2$O$_3$ progresses more efficiently than the urea incubation method. Thus, this is a potential method that can be applied to rubber industry.

4. Conclusion

The crystallite sizes of CFO and CFO@Al$_2$O$_3$ are 27.3 nm and 56.2 nm, evenly distributed. CFO@Al$_2$O$_3$ surface (600°C, 2h) reaches 216.75 m^2/g, has pores from 30-120Å and pore volume of 0.5-1 cm^3/g. VSM measurement results show that the saturation of CFO@Al$_2$O$_3$ is lower than that of uncoated Al$_2$O$_3$ CFO. Research on CFO@Al$_2$O$_3$ nanomaterial for protein separation in natural rubber has been successful, removing up to 96.71% protein under specific conditions: CFO@Al$_2$O$_3$ (600°C, 2h), %SDS=0.1wt.%, pH = 11, %NPs = 1 wt.%, t = 60 minutes, %DRC = 10%.

The next development direction could be applying the protein removal method using CFO@Al$_2$O$_3$ nanoparticles on an industrial scale, combined with the urea method to separate proteins in the most effective way.

References

[1] J. W. Yunginger, R. T. Jones, A. F. Fransway, J. M. Kelso, M. A. Warner, and L. W. Hunt, Extractable latex allergens and proteins in disposable medical gloves and other rubber products, Journal of Allergy Clinical Immunology vol. 93, no. 5, pp. 836-842, 1994.
https://doi.org/10.1016/0091-6749(94)90374-3

[2] J. D. Katz *et al.*, Natural rubber latex allergy: Considerations for anesthesiologists, American Society of Anesthesiologists, vol. 847, 2005.

[3] C. Nakason, A. Kaesaman, and N. Yimwan, Preparation of graft copolymers from deproteinized and high ammonia concentrated natural rubber latices with methyl methacrylate, Journal of Applied Polymer Science, vol. 87, no. 1, pp. 68-75, 2003.
https://doi.org/10.1002/app.11671

[4] Y. Yamamoto, P. T. Nghia, W. Klinklai, T. Saito, and S. Kawahara, Removal of proteins from natural rubber with urea and its application to continuous processes, Journal of Applied Polymer Science, vol. 107, no. 4, pp. 2329-2332, 2008.
https://doi.org/10.1002/app.27236

[5] B. Issa, I. M. Obaidat, B. A. Albiss, and Y. Haik, Magnetic nanoparticles: surface effects and properties related to biomedicine applications, International journal of molecular sciences, vol. 14, no. 11, pp. 21266-21305, 2013.
https://doi.org/10.3390/ijms141121266

[6] M. Trueba and S. P. Trasatti, γ-Alumina as a support for catalysts: a review of fundamental aspects, European journal of inorganic chemistry, vol. 2005, no. 17, pp. 3393-3403, 2005.
https://doi.org/10.1002/ejic.200500348

[7] M. G. Naseri, E. B. Saion, H. A. Ahangar, A. H. Shaari, and M. Hashim, Simple synthesis and characterization of cobalt ferrite nanoparticles by a thermal treatment method, Journal of Nanomaterials, vol. 2010, pp. 1-8, 2010.
https://doi.org/10.1155/2010/907686

[8] N. T. Thuong, P. T. Nghia, and S. Kawahara, Removal of proteins and its effect on molecular structure and properties of natural rubber, JST: Engineering and Technology for Sustainable Development, vol. 32, no. 2, pp. 008-015, 2022.
https://doi.org/10.51316/jst.157.etsd.2022.32.2.2